



Experiments Using a Design-for-Manufacturing Approach to Process Parameters for Fused Deposition Modelling.

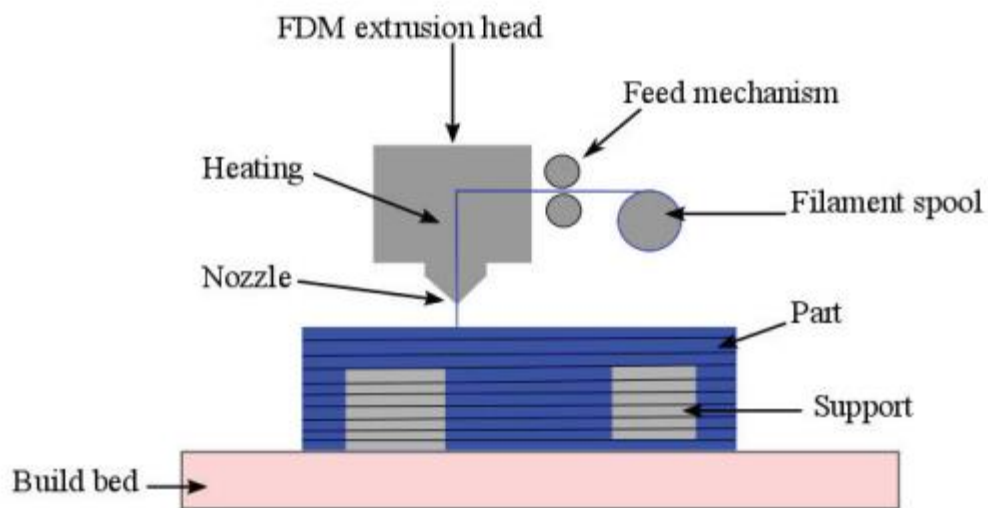
*BANTU SAILESH 1, R HARI KRISHNA 2,
ASSOCIATE PROFESSOR 1, ASSISTANT PROFESSOR 2,
Mail ID: sailesh.bantu04@gmail.com, Mail ID: ramagirihari345@gmail.com
Dept.: Mechanical
Pallavi Engineering College,
Kuntloor(V), Hayathnagar(M), Hyderabad, R.R. Dist. - 501505.*

Abstract

As a quick prototyping method for visualising and validating ideas, additive manufacturing (AM) first emerged. As AM technologies like Fused Deposition Modeling (FDM) have advanced in recent years, they are now moving from fast prototyping to rapid production applications. The issue of manufacturing usable components for end-users utilising FDM proved to be a difficult one. Building direction, extrusion temperature, layer height, infill pattern and more are just few of the many variables that determine the final design of a component. Quality and functionality are influenced by the FDM process parameters. Detailed knowledge of the effects of the FDM processing settings on the mechanical qualities, dimensional accuracy, and construction time of the finished product is also needed. When it comes to the mechanical qualities and repeatability of FDM components, an experimental research has been conducted to examine the impact of each processing parameter. 18 test samples were printed using different processing conditions. It was necessary to measure the measurements of these specimens and compare them to an accurate 3D CAD model to examine the repeatability and the resulting tolerances. To determine the mechanical parameters of each produced sample, the research described here used an ASTM D638 tensile test. A Finite Element Analysis (FEA) model is also included in the paper. Future studies on the combined impacts of processing parameters should include simulating their behaviour under mechanical stresses.

Introduction

There are many different types of advanced manufacturing technologies, and AM is the general word for all of them. By adding material rather than removing it as in subtractive manufacturing methods like milling, the layers are created. G-codes created from 3D CAD models regulate the addition or fusion of materials. Formed by heating a thermoplastic filament to a semi-liquid condition and extruding it via an extruding nozzle, FDM is one of the AM methods that manufactures components layer by layer. In most FDM systems, the filament has a circular cross section and a particular diameter. 1.75 mm and 3.0 mm are the most often utilised sizes. Many benefits occur because of the nature of the FDM process, such as the design flexibility to make complicated forms without the need to invest in dies and moulds, the capacity to generate interior features, which is unachievable using conventional manufacturing processes. Consolidated complicated pieces may reduce the number of assemblies produced using FDM. Reduced lead times and storage and shipping requirements, particularly in applications requiring high levels of customisation, are further benefits of FDM that may be realised across the supply chain [2]. Aside from these drawbacks (such as anisotropic mechanical characteristics, staircase effect at curved surfaces, poor surface quality, the necessity for supports for overhanging portions), FDM technique offers several advantages. Many academics are working to improve the quality of FDM components in order to address these issues. Many methods exist for enhancing the quality of additive manufacturing (AM) and fused deposition modelling (FDM) components, including chemical treatment (3–6), machining (7–8), heat treatment (9), and parameter optimization).



Since lowering post-processing is an objective of AM, the research has focused on optimising processing parameters. Processing parameters may be optimised by conducting experiments or modelling them in a computer simulation. The Taguchi approach [10–12], complete factorial designs [13–15], ANOVA [16], the bacteria forging technique [17], and fuzzy logic [19] have all been applied to improve processing parameters. A wide range of processing parameters were examined in these investigations. Building direction [20] is an example of one processing parameter that has been comprehensively explored in one publication. Other studies, however, analyse the impacts of three or four processing factors simultaneously, such as layer height [15], building direction [18], and raster angle [21]. There are normally two or three layers of investigation for each parameter in the second technique. On the other side, FEA is the most used approach for simulating a design. Modeling FDM pieces as orthotropic materials allowed Domingo-Espin et al. [22] to mimic the influence of building direction on mechanical behaviour. For components with low infill percentages, Farbman & McCoy [23] approximated the influence of infill pattern on mechanical characteristics by adding the infill features to the simulated CAD model. No matter how much

research has already been done on the subject, there is still a dearth of information that explains how to design FDM components with high repeatability and dimensional accuracy, despite several published studies on this subject. That's why we need some kind of systematic method for examining the impact of processing factors. In order to have a better knowledge of the impacts of each parameter, this study examines them independently at a greater number of levels than earlier studies. Using a novel methodology based on the relative density of printed components to generate voids or porosities, this study modifies the FEA model for FDM parts and compares it to actual data and another simulation method. Second, the methodological approach

Sample preparation

The plastic tensile testing specimens utilised in this investigation were modelled after American Society for Testing and Materials ASTM D638 type IV standards for dimensional accuracy, repeatability, and mechanical characteristics. These measurements were utilised to generate a CAD model seen in Figure 2. A Makerbot Replicator 2X 3D printer was used to produce all of the specimens.

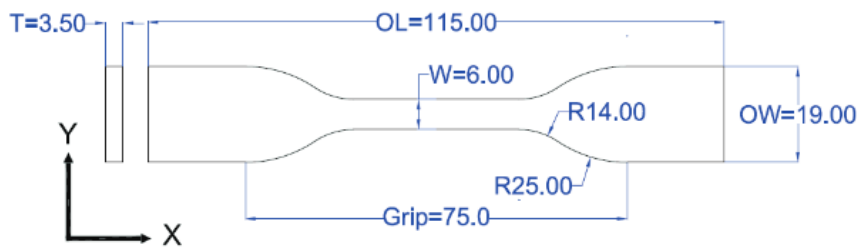


Figure 2: Created specimens' CAD model, dimensions in mm

In a separate study, the impacts of six processing factors on mechanical qualities, dimensional accuracy, and repeatability were analysed. As a result, in each faked sample, the value of just one processing parameter was altered. printing speed, and extrusion direction were all factors that had to be taken into account while designing Infill percentage, layer height, and infill patterns all have a role. The building's axis displays the normal vector to the building. The axis in Figure 2 was used to guide the printing of the layers. Creating samples in the direction of construction Z, for example, is equivalent to saying that the printed layers are perpendicular to the x-y coordinate plane. The percentage of infill reflects the density of the printed object. a portion of the object that is neither a shell nor solid. A 3D printer's extrusion temperature and printing

speed both affect the speed at which the heated filament is extruded from the nozzle. The thickness of each layer is determined by the height of the layer. This is all accomplished by modifying the nozzle's infill patterns. Linear, diamond, and hexagonal infill designs were employed in this research, where Diamond F has the same geometry as the Diamond infill pattern, but uses quicker printing G codes owing to the difference in partitioning of the pattern itself. However, the extruder is subjected to larger stresses for suddenly shifting directions with this quicker printing pattern. Table 1 shows the results of an investigation into each of these processing variables on a four-level scale. However, there were only three possible construction directions.

Ala'aldin Alafaghani et al. / Procedia Manufacturing 10 (2017) 791 – 803

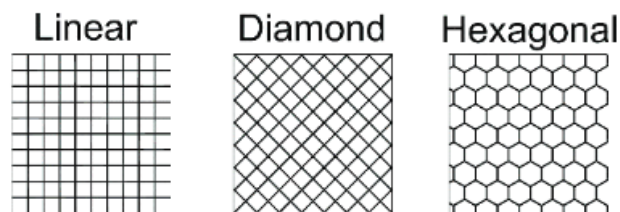


Figure 3: Infill patterns shape schematic

Table 1: The Values of varying Processing Parameters.

Levels	Building Direction	Infill Percent	Print Speed	Extrusion Temperature	Layer Height	Infill Pattern
0 (Reference)	Z	100	90 mm/s	185 C ^o	0.30 mm	(1) Diamond F
1	X	20	70 mm/s	175 C ^o	0.10 mm	(2) Diamond
2	Y	50	120 mm/s	180 C ^o	0.25 mm	(3) Linear
3	Z	80	170 mm/s	205 C ^o	0.40 mm	(4) Hexagonal



We devised an experiment to make a total of 18 samples based on the values provided in Table 1. Table 2 shows the specifics of how each sample was processed. For each sample, the bolded values show which processing parameter is most important. In order to study the influence of repeatability on the mechanical properties and

dimensional accuracy of each sample, three specimens were made. Changing numerous parameters at the same time isn't possible in this study since only one parameter is changed at a time. However, this is clearly the future course of action for the company.

Table 2 Sample processing parameters specification

Sample	Building Direction	Infill Percent	Print Speed	Extrusion Temperature	Layer Height	Infill Pattern
1	X	100	90 mm/s	185 C ^o	0.30 mm	Diamond (F)
2	Y	100	90 mm/s	185 C ^o	0.30 mm	Diamond (F)
3	Z	100	90 mm/s	185 C ^o	0.30 mm	Diamond (F)
4	Z	20	90 mm/s	185 C ^o	0.30 mm	Diamond (F)
5	Z	50	90 mm/s	185 C ^o	0.30 mm	Diamond (F)
6	Z	80	90 mm/s	185 C ^o	0.30 mm	Diamond (F)
7	Z	100	170 mm/s	185 C ^o	0.30 mm	Diamond (F)
8	Z	100	120 mm/s	185 C ^o	0.30 mm	Diamond (F)
9	Z	100	70 mm/s	185 C ^o	0.30 mm	Diamond (F)
10	Z	100	90 mm/s	175 C^o	0.30 mm	Diamond (F)
11	Z	100	90 mm/s	180 C^o	0.30 mm	Diamond (F)
12	Z	100	90 mm/s	205 C^o	0.30 mm	Diamond (F)
13	Z	100	90 mm/s	185 C ^o	0.40 mm	Diamond (F)
14	Z	100	90 mm/s	185 C ^o	0.25 mm	Diamond (F)
15	Z	100	90 mm/s	185 C ^o	0.10 mm	Diamond (F)
16	Z	100	90 mm/s	185 C ^o	0.30 mm	Diamond
17	Z	100	90 mm/s	185 C ^o	0.30 mm	Linear
18	Z	100	90 mm/s	185 C ^o	0.30 mm	Hexagonal

Influence of processing parameters on dimensional accuracy repeatability

All printed specimens were measured and compared to the planned CAD model in order to assess the impact of processing settings on dimensional accuracy and repeatability. Nine measurements were taken for each specimen, including the overall length (OL), the whole breadth, the thickness (T), and the width (W) of

the reduced section as shown in Figure 3. Using a Vernier calliper, the length of the piece was determined. A micrometre was used to determine the remaining dimensions. The average of the three width measurements, W1, W2, and W3, yielded a single value, W. The remainder of the data was averaged in the same way.

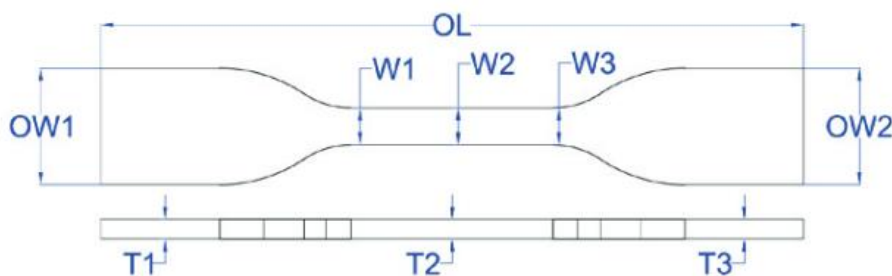


Figure 4: Measurement locations of the FDM specimens



Mechanical Properties

The specimens were tested according to ASTM D638-15 standards using an Instron 3369 universal testing equipment in order to assess the mechanical qualities of the FDM components. At room temperature, an extension speed of 5 mm/min was used to manage the testing pace. Extensometers were used to capture real-time data throughout the testing, including load, extension, strain, and time. The following mechanical characteristics were computed based on the gathered data: Tensile strength, yield stress, Young's Modulus, and ductility are all characteristics to consider. Accordingly, the stresses and mechanical characteristics of each specimen are estimated taking into account any dimensional inaccuracies.

Finite Element Analysis

As seen in Figure 5's Scanning Electron Microscope (SEM) picture, FDM components even at 100% infill exhibit gaps and porosities, therefore this research provides a novel FEA technique that exploits the apparent density of FDM parts to create a functional model for future analysis (a) Weight was used to determine the specimen's mass, and water displacement was used to determine its volume. Appearance density was computed by multiplying the mass by the volume. Sample 3 was chosen to compare the outcomes of the other specimens since it was made using all of the reference processing settings. In addition, the FEA made use of sample 3's experimental data as a source of reference. The mechanical qualities of the initial PLA filament, as determined by the previous tensile test, were measured in terms of material properties. Table 3 summarises the findings of the measurements for both sample 3 and PLA filament. 1.75 mm filaments were employed in this investigation.

Table 3 Physical properties of sample 3 and PLA material

Sample	Volume [cm ³]	Mass [g]	Apparent Density [g/cm ³]	Yield stress [MPa]	Load at yield [N]	Strain at yield [mm/mm]	Young's modulus [MPa]
Sample 3	5.05	5.91	1.15	40.09	877.9	0.01442	3144.19
PLA Filament	3.19	3.99	1.25	49.72	111.52	0.01401	3787.08

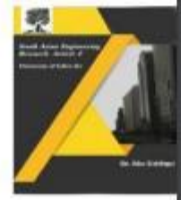
Modeling FDM components in FEA requires taking into account any gaps or voids that may exist in the CAD model. Material discontinuities caused by layer fusion in the CAD model for FEA were calculated using the difference in density. The diamond infill pattern and a raster angle of 45 degrees were used to determine the

geometry of the discontinuities, which had lengths of 0.2 mm x 0.2 mm. This size was employed to save calculation time and lessen the requirement for finer meshing, even though discontinuities in the real FDM component are considerably smaller. Equation is used to introduce the number of holes per area (HPA).

$$\rho_{FDM} = (V_{CAD} \times \rho_{Filament} - \rho_{Filament} \times l^2 \times T \times A_{CAD} \times HPA) / V_{CAD}$$

An FDM part's FDMU is the apparent density of its material; CADV is its volume, and FilamentU is its density (Table 3). Discontinuity length is 0.20 mm. The specimen's area is represented in Figure 2 as its area in X-Y. In Equation 1 the HPA was determined to be 1.9998 holes /mm² by inserting these values. As a result, around 300 holes in the 25 mm x 6 mm gauge length area are required. If you want a more realistic model, you may shorten l and raise HPA, but this requires a

finer mesh and so increases simulation time. Symmetry around Y-axis was employed to save calculation time and just the upper half of the specimen was modelled with holes as illustrated in Figure (b). Sample 3's yield load of 877.9 N was split across the area of the grip sides and applied to the other grip sides under a distributed load with a fixed boundary condition on one of the grip's sides. With a Poisson's ratio of 0.35, the filament was considered to be isotropic and



fine mesh was placed to the gauge length region with the holes in order to simulate its mechanical characteristics. Unfortunately, the simulated model expects homogeneous attributes throughout the layers, which is not the case. The previously mentioned model was used in a second FEA example. However, the fusion effect cannot be compensated for without it (i.e. voids). Because the density ratio between sample 3 and the filament is 0.92, the mechanical properties of

the filament were multiplied by that density to arrive at the final mechanical characteristics of the model. Gage length area average strain was determined from average displacement for two sections divided by the original distance between them in order to validate simulation results. Figure 5 is an example of what I mean. a) SEM images of the tested FDM specimen. b) CAD simulation model with discontinuities in the materials.

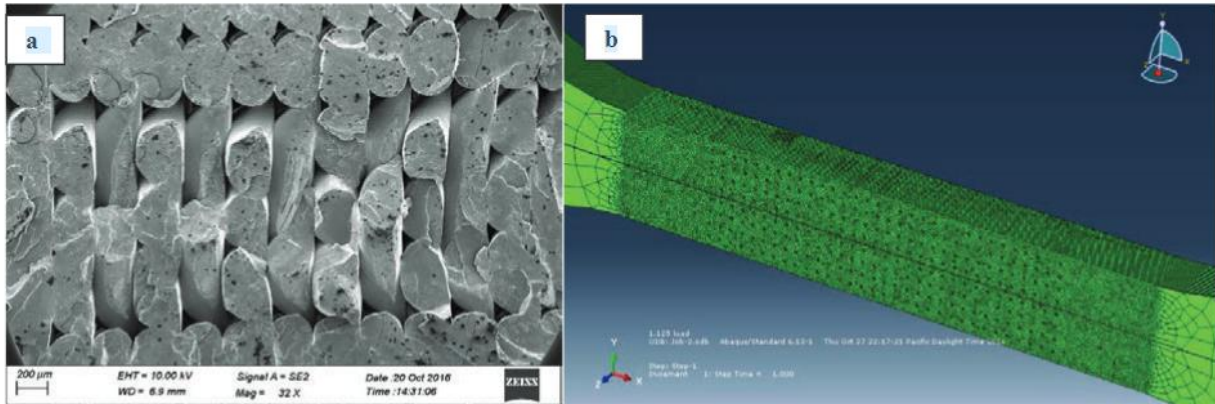


Figure 5: a) SEM of tested FDM specimen. b) Simulation CAD model with material discontinuities.

Results and Analysis

The precision and repeatability of dimensional measurements Each sample's width was calculated by averaging its three width measurements (W1, W2, and W3). For the OW1 and OW2 and OT1, OT2, and OT3 measurements of overall width and thickness, the

same procedure was used. Table 4 displays the findings of these tests. For example, OL= 115.0mm for overall length, OW=19.00mm for overall width, W=6.00mm reduced section width and T =3.50mm thickness were measured and compared to the design parameters. A faulty equation was used to construct the figure



$$Error = Measured Value - Design Value \quad (2)$$

Table 4 Samples measurements averaged results, dimensions in mm.

Specimen Number	Overall Length	Overall Width	Reduced Section Width	Thickness
CAD Model	115.00	19.00	6.00	3.50
1	115.08	18.98	5.95	4.12
2	114.58	18.73	6.55	3.72
3	114.51	19.29	6.44	3.93
4	114.58	19.21	6.36	3.74
5	114.51	19.24	6.28	3.70
6	114.67	19.29	6.42	3.72
7	114.59	19.24	6.35	3.74
8	114.66	19.21	6.30	3.75
9	114.76	19.27	6.31	3.71
10	114.64	19.17	6.27	3.56
11	114.61	19.35	6.33	3.72
12	114.74	19.30	6.46	3.95
13	114.68	19.48	6.48	3.84
14	114.48	19.17	6.18	3.59
15	114.99	18.81	6.27	3.56
16	114.69	19.34	6.36	3.74
17	114.66	19.29	6.43	3.71
18	114.64	19.31	6.38	3.74

From Figure 6-a it is clear that the building direction affects the dimensional accuracy significantly. The first observation is that most of the errors have positive values, which indicates that the printer tends to create larger components than anticipated. However, even if it is difficult to draw patterns of how building direction influences the mistake in dimensions, it is apparent that the dimensional accuracy is impacted by the construction direction. That may be due to the fact that the extruder on the Makerbot 2X has a positioning resolution of 11 microns in the layer plane and 2.5 microns in the construction direction, as stated by the manufacturer. In addition, the height of the component must be an integer number of layer thicknesses, but the plane dimensions are more connected to the extruder positioning precision and the nozzle diameter. According to Figure 6-b and 6-d, the dimensional inaccuracy is not affected by infill % or infill patterns. Because of this, the diamond rapid infill pattern has resulted

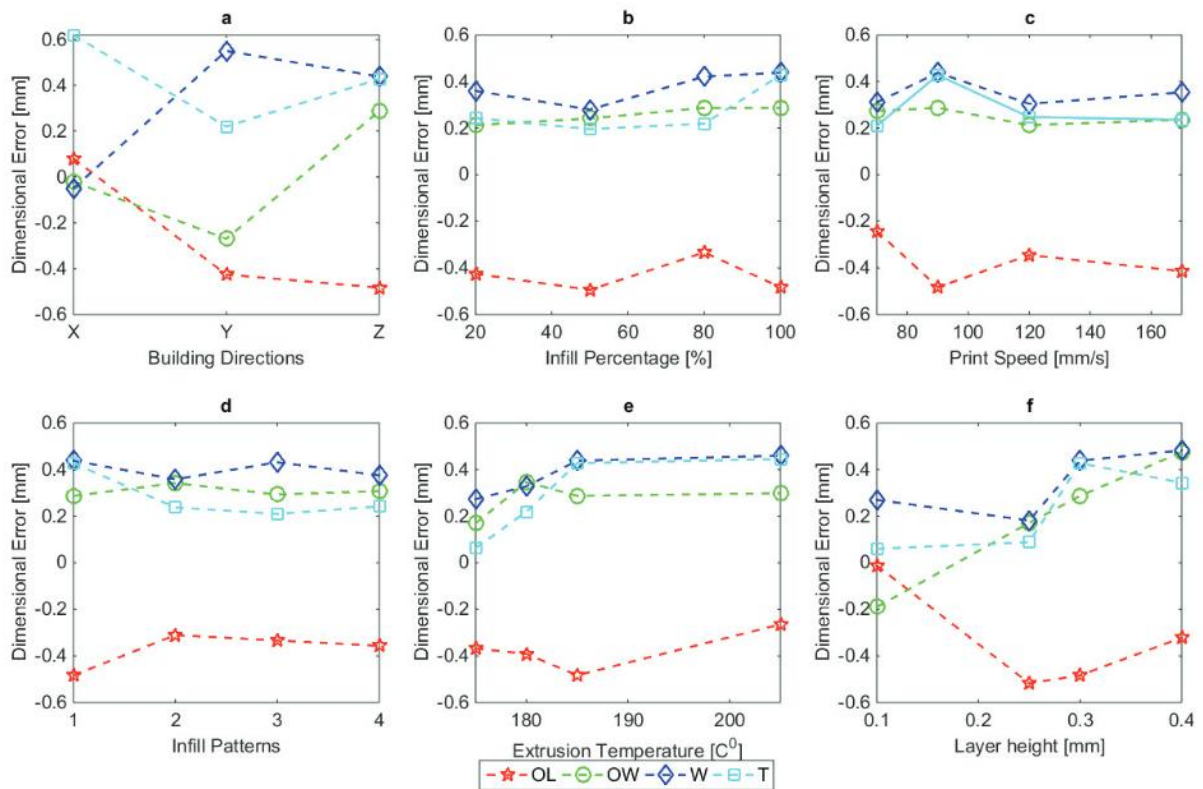
in more thickness errors, which is the most critical dimension. Only at printing speeds of 90 mm/s did the errors in all tested dimensions remain consistent, as shown in Figure 6-c. Because the rise in error only happened at one printing speed, there were no distinct trends, the thickness and the width at the decreased section rose from 0.31 to 0.44mm roughly for the reduced width and from 0.21 to 0.43mm for the thickness. When printing at such a high rate of speed, a unique heat transfer or temperature gradient may be responsible for this phenomena. Printing rates typically vary from 40mm/s to 80mm/s, although this should be noted. As the extrusion temperature rises, so does the error seen in Figure 6-e, which may be related to the increased fluidity of the extruded filament at a higher temperature, allowing it to flow out of the nozzle control and so increasing the mistake. The importance of layer height in terms of dimensional precision and resolution is well established [24] Figure 6-f shows that in general,



lower layer heights result in reduced errors. There was a minor amount of slack even when the layer height was identical to 0.25 mm. This may be explained by the fact that $T=3.50$ mm is an integer multiple of 0.25 mm, hence the mistake in thickness was minimal. That explains the spike in inaccuracy that occurs when the layer is raised to 0.30 mm in thickness. When comparing many dimensions at the same time, absolute changes in dimensions may be preferable since the total length error and its variations are minor when compared to the

mistakes of the other dimensions if the error was stated as a percentage error.

Building direction, infill percentage, printing speed, extrusion temperature and layer height all contribute to dimensional inaccuracy [percentage]. 3.2. Results and analysis of mechanical characteristics The same method used to investigate dimensional accuracy was used in this investigation. Table 5 displays the averaged results of the tensile tests. Figure 7 is based on the data shown in this section.



Results and analysis of mechanical characteristics

The same method used to investigate dimensional accuracy was used in this investigation. Table 5 displays the averaged results of the tensile tests. Figure 7 is based on the data shown in this section. Figure 7 indicates that processing settings have a significant impact on the mechanical characteristics. As shown in Figure 7 -a, the Young's modulus, tensile strength, and yield strength are all lower when

the structure is built in the X direction than when it is in the Y or Z directions. [25] The results of the building direction are consistent with earlier research. This suggests that the bonding or fusion between layers is weaker than in the individual layers. As a consequence, subsequent extruded routes fuse better because of their mutual high temperature, but subsequent layers often have a greater temperature gradient, limiting the adhesion between the layers and creating a weaker piece. It is possible that the difference in strength and stiffness between Y and Z construction directions is due to the fact



that the Z building direction has a lower number of layers, which interprets the greater strength in Z direction. Figure 7-b shows that increasing the infill percentage improves the mechanical characteristics as predicted. Higher infill percentages enhanced mechanical characteristics by giving more material to take the stresses given by the tensile machine, while the infill % cannot be directly equated to the weight percentage of the specimen to the completely filled specimen. Figures 7-c and 7-d illustrate that printing speed and infill patterns have no effect on mechanical characteristics. There is some evidence to suggest that infill patterns influence mechanical qualities, however [26],

[27]. As a result of printing components with varied infill patterns at a 100% infill percentage, which is intended to lessen their impact on mechanical characteristics, the infill patterns' relative independence from mechanical qualities may be explained. The impact of infill patterns can only be clearly seen in bigger specimens with smaller infill percentages. Figure 7-e shows the influence of extrusion temperature. The mechanical qualities improved as the temperature rose, which may be attributed to the enhanced fusing of the extruded layer and the layers that surround it. Increasing the extrusion temperature beyond a certain point yields little benefit, as can be seen in the graph.

Table 5: Tensile testing results

Sample Number	Young's Modulus [MPa]	Sy 0.001 offset [MPa]	Tensile Strength [MPa]	Ductility [mm/mm]
1	2608.80	35.11	42.12	0.019010
2	2815.58	37.22	45.72	0.019190
3	3144.19	40.09	46.06	0.019633
4	2851.84	38.53	42.95	0.024780
5	2240.56	30.00	34.39	0.026593
6	2255.35	28.83	33.74	0.020033
7	2837.48	38.67	42.98	0.028873
8	2950.99	38.80	43.65	0.026807
9	2803.19	38.79	43.25	0.028623
10	1947.05	25.37	28.59	0.019040
11	2581.47	34.65	40.58	0.026373
12	3004.46	39.39	43.79	0.019667
13	3177.53	35.32	46.10	0.021803
14	2599.09	31.02	43.17	0.025797
15	2586.30	29.31	39.19	0.020920
16	2810.19	38.26	43.61	0.025470
17	2834.32	37.77	43.57	0.026600
18	2859.27	39.47	44.75	0.028100

Figure 7 shows that raising the layer height improves mechanical characteristics. That lends credence to the idea that fewer layers result in structurally sound components. When layer height is increased from 0.30 to 0.40 mm, the figure indicates no improvement in the yield strength and Young's modulus. For ductility, there are no obvious correlations. There was also a significant degree of consistency in yield strength, tensile strength, and Young's modulus across the specimens in the same sample,

although a large degree of variability was found in ductility.

FEA results and analysis

Figure 8 shows the findings of the first material discontinuity FEA model. As seen in Figure 8, the breaking pattern around the raster lines in the test specimens is caused by a buildup of tension around the holes. The simulation's highest stress of 55.97 MPa is higher than the filament's yield

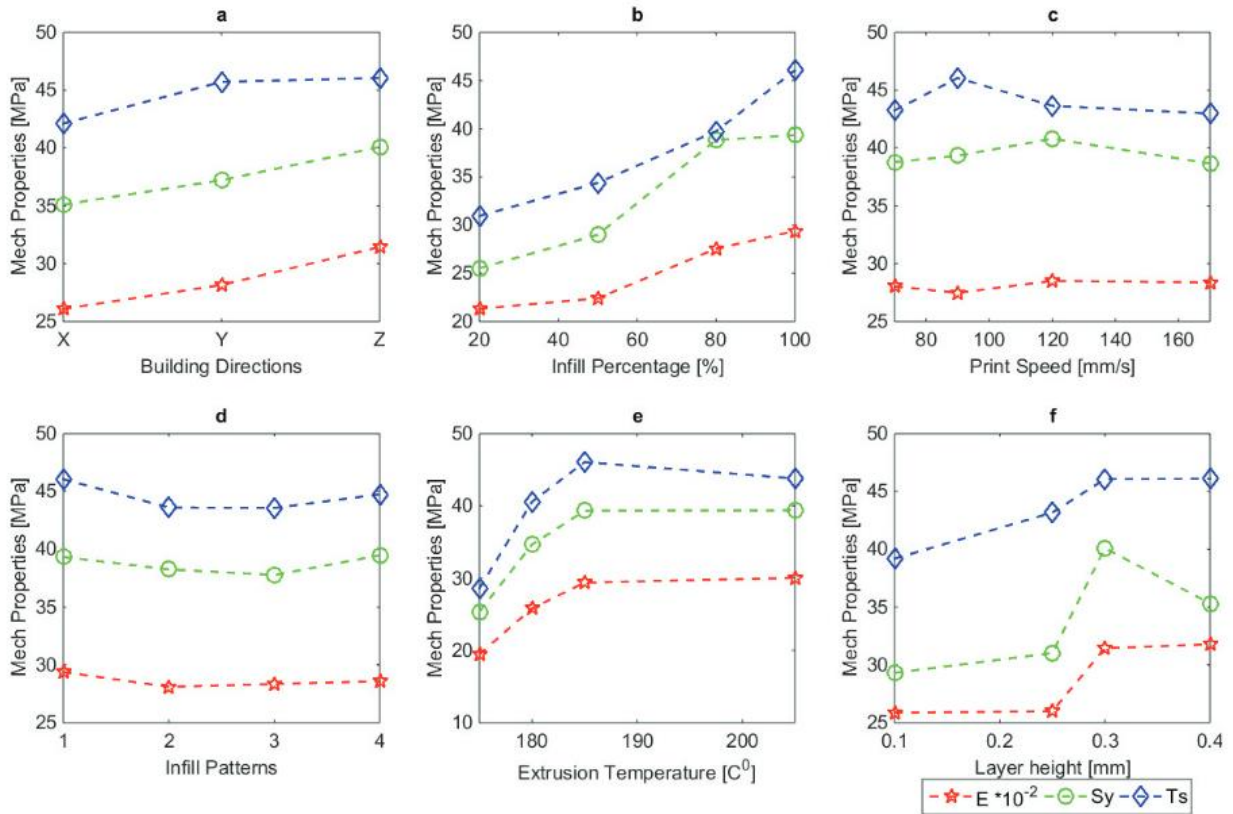


stress of 46.90 MPa in the experiment. A typical strain of 0.012715 with an inaccuracy of 9.2434 percent is found in the gauge area, which is quite similar to the experimental values. It is shown in Figure 8 that a first simulation was run using the Von Mises stress and principal strain contours. Both samples 3 and 4 showed similar results in their yield stress measurements in the second simulation (43.48% and 40.9%, respectively). There was a 19.0% inaccuracy in the tensile test on sample 3, although the average strain was 0.01167. Results from both simulations are similar. The second FEA model is less computationally intensive, but it does not explain

the tensile specimens' breaking pattern, as can be seen in Figure 9 of the first FEA model.

(a) building direction, (b) infill %, (c) printing speed, and (d) infill patterns all affect mechanical characteristics [MPa] as shown in Figure 7.

E stands for the Young's modulus, S_y for the yield strength, and T_s for the tensile strength, while layer height (e) and extrusion temperature (f) round out the equation.



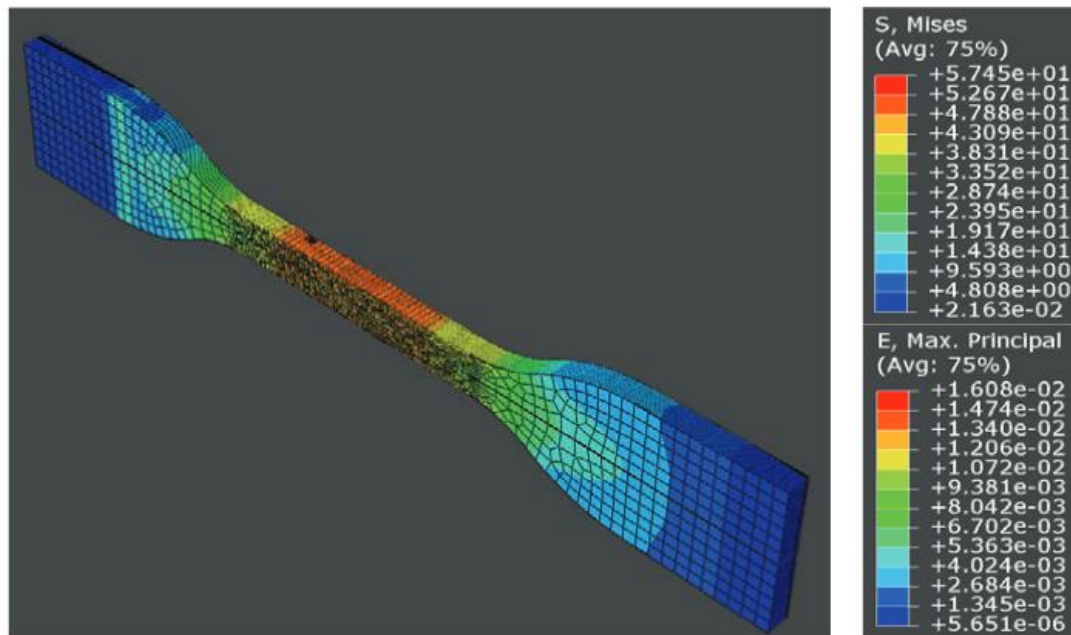


Figure 8: Von Mises stress distribution on the model with discontinuities with legends of Von Mises and principle strain.

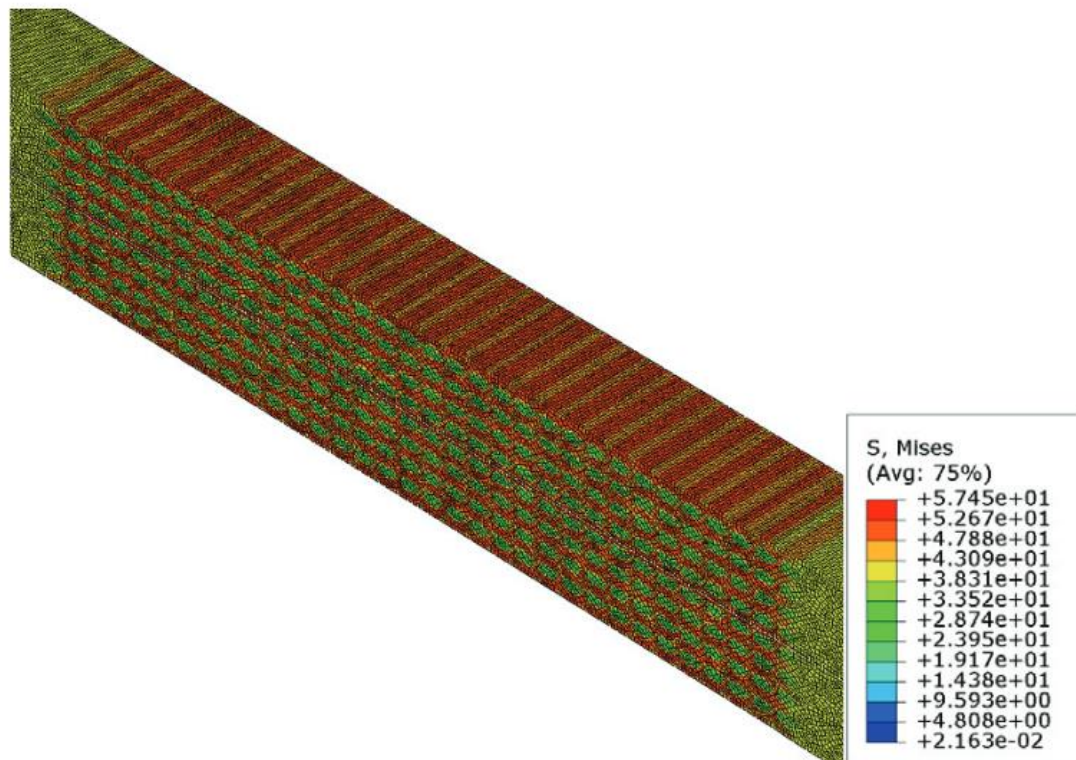


Figure 9: Von Mises stress concentration around discontinuities.

Conclusion

Here, we look see how final product qualities are influenced by various FDM processing factors. The research explores the influence on mechanical qualities and dimensional accuracy of building orientations, infill percentages, infill patterns, print speeds, extrusion temperatures, and layer height separately. In addition, a newly developed technique to modelling FDM components using FEA is presented in the paper. More than infill %, infill pattern, and printing speed, it was found that building direction extrusion temperature and layer height had the greatest impact on dimensional accuracy. For FDM products, it is generally recommended that the critical dimension should be parallel to the layer orientation rather than the construction direction, in addition to decrease extrusion temperature and layer height, to increase dimensional accuracy. Layer height and infill patterns, for high infill percentages

References

specimens, and printing speed had less of an impact on mechanical qualities than building direction, extrusion temperature, and layer height. In order to increase mechanical qualities, greater extrusion temperatures and higher layer heights are required, as well as a suitable construction direction that aligns the layers with the direction of load. Greater specimens with lower infill percentages are needed in order to show the relevance of patterns of infilling. There are encouraging results in both ways employing density ratio between filament and FDM component. However, it is necessary to increase the impact of layers. Building on this work, future research should focus on infill patterns with lower infill percentages, on the effects of other processing parameters like cooling rate and environmental conditions, and on investigating the combined effect of multiple processing parameters at multiple levels when applied to larger specimens. Replace isotropic attributes with lamia ones to simulate the model.



- [1] K. J. De Laurentis and C. Mavroidis, "Rapid fabrication of a nonassembly robotic hand with embedded components," *Assem. Autom.*, vol. 24, no. 4, pp. 394-405, Dec. 2004.
- [2] D. Thomas and S. Gilvert, "Costs and Cost Effectiveness of Additive Manufacturing," *US Dep. Commer.*, no. December, 2014.
- [3] L. M. Galantucci, F. Lavecchia, and G. Percoco, "Experimental study aiming to enhance the surface finish of fused deposition modeled parts," *CIRP Ann. - Manuf. Technol.*, vol. 58, no. 1, pp. 189-192, 2009.
- [4] L. M. Galantucci, F. Lavecchia, and G. Percoco, "Quantitative analysis of a chemical treatment to reduce roughness of parts fabricated using fused deposition modeling," *CIRP Ann. - Manuf. Technol.*, vol. 59, no. 1, pp. 247-250, 2010.
- [5] A. Garg, A. Bhattacharya, and A. Batish, "Chemical vapor treatment of ABS parts built by FDM: Analysis of surface finish and mechanical strength," *Int. J. Adv. Manuf. Technol.*, pp. 1-17, 2016.
- [6] V. Tiwary, P. Arunkumar, A. S. Deshpande, and V. Khorate, "Studying the effect of chemical treatment and fused deposition modeling process parameters on surface roughness to make acrylonitrile butadiene styrene patterns for investment casting process," *Int. J. Rapid Manuf.*, vol. 5, no. 3-4, pp. 276-288, 2015.
- [7] P. M. Pandey, N. Venkata Reddy, and S. G. Dhande, "Improvement of surface finish by staircase machining in fused deposition modeling," *J. Mater. Process. Technol.*, vol. 132, no. 1, pp. 323-331, 2003.
- [8] O. Kerbrat, P. Mognol, and J. Y. Hasco??t, "A new DFM approach to combine machining and additive manufacturing," *Comput. Ind.*, vol. 62, no. 7, pp. 684-692, 2011.
- [9] J. F. Rodríguez, J. P. Thomas, and J. E. Renaud, "Mechanical behavior of acrylonitrile butadiene styrene (ABS) fused deposition materials. Experimental investigation," *Rapid Prototyp. J.*, vol. 7, no. 3, pp. 148-158, Aug. 2001.
- [10] R. Anitha, S. Arunachalam, and P. Radhakrishnan, "Critical parameters influencing the quality of prototypes in fused deposition modelling," *J. Mater. Process. Technol.*, vol. 118, no. 1-3, pp. 385-388, 2001.
- [11] J. S. Chohan and R. Singh, "Enhancing dimensional accuracy of FDM based biomedical implant replicas by statistically controlled vapor smoothing process," *Prog. Addit. Manuf.*, vol. 1, no. 1, pp. 105-113, 2016.
- [12] C. C. Wang, T. Lin, and S. Hu, "Optimizing the rapid prototyping process by integrating the Taguchi method with the Gray relational analysis," *Rapid Prototyp. J.*, Apr. 2013.
- [13] S.-H. Ahn, M. Montero, D. Odell, S. Roundy, and P. K. Wright, "Anisotropic material properties of fused deposition modeling ABS," *Rapid Prototyp. J.*, vol. 8, no. 4, pp. 248-257, 2002.
- [14] K. Chin Ang, K. Fai Leong, C. Kai Chua, and M. Chandrasekaran, "Investigation of the mechanical properties and porosity relationships in fused deposition modelling fabricated porous structures," *Rapid Prototyp. J.*, vol. 12, no. 2, pp. 100-105, Mar. 2006.
- [15] G. C. Onwubolu and F. Rayegani, "Characterization and Optimization of Mechanical Properties of ABS Parts Manufactured by the Fused Deposition Modelling Process," *Int. J. Manuf. Eng.*, vol. 2014, p. 13, 2014.
- 803Ala'aldin Alafaghani et al. / *Procedia Manufacturing* 10 (2017) 791 - 803
- [16] B. H. Lee, J. Abdullah, and Z. A. Khan, "Optimization of rapid prototyping parameters for production of flexible ABS object," *J. Mater. Process. Technol.*, vol. 169, no. 1, pp. 54-61, 2005.
- [17] T. Nancharaiyah, "Optimization of Process Parameters in FDM Process Using Design of Experiments," *Optimize*, vol. 2, no. 1, pp. 100-102, 2011.
- [18] S. K. Panda, "Optimization of Fused Deposition Modelling (FDM) Process Parameters Using Bacterial Foraging Technique," *Intell. Inf. Manag.*, vol. 1, no. 2, pp. 89-97, 2009.
- [19] Ranjeet Kumar Sahu, S.S. Mahapatra, Anoop Kumar Sood "A Study on Dimensional Accuracy of Fused Deposition Modeling (FDM) Processed Parts using Fuzzy Logic," *Journal for Manufacturing Science & Production*, vol. 13, p. 183, 2013.
- [20] K. Thrimurthulu, P. M. Pandey, and N. Venkata Reddy, "Optimum part deposition orientation in fused deposition modeling," *Int. J. Mach. Tools Manuf.*, vol. 44, no. 6, pp. 585-594, 2004.
- [21] K. P. K. Vishal N. Patel, "Parametric Optimization of The Process of Fused Deposition Modeling In Rapid Prototyping Technology- A Review," *Int. J. Innov. Res. Sci. Technol.*, vol. 1, no. 7, pp. 80-82, 2014.
- [22] M. Domingo-Espin, J. M. Puigoriol-Forcada, A. A. Garcia-Granada, J. Llumà, S. Borros, and G. Reyes, "Mechanical property characterization and simulation of fused deposition modeling Polycarbonate parts," *Mater. Des.*, vol. 83, pp. 670-677, 2015.
- [23] M. Farbman, Daniel, Chris, "Materials Testing of 3D Printed ABS and PLA Samples to Guide Mechanical Design," pp. 1-12, 2016.
- [24] P. M. Pandey, N. V. Reddy, and S. G. Dhande, "Real time adaptive slicing for fused deposition modelling," *Int. J. Mach. Tools Manuf.*, vol. 43, no. 1, pp. 61-71, 2003.
- [25] O. S. Es-Said, J. Foyos, R. Noorani, M. Mendelson, R. Marloth, and B. A. Pregger, "Effect of Layer Orientation on Mechanical Properties of Rapid Prototyped Samples," *Mater. Manuf. Process.*, vol. 15, no. 1, pp. 107-122, 2000.
- [26] B. M. Tymrak, M. Kreiger, and J. M. Pearce, "Mechanical properties of components fabricated with open-source 3-D printers under realistic environmental conditions," 2014.
- [27] A. K. Sood, R. K. Ohdar, and S. S. Mahapatra, "Parametric appraisal of mechanical property of fused deposition modelling